Wetzel, M., Kempka, T., Kühn, M. (2017): Predicting macroscopic elastic rock properties requires detailed information on microstructure. - *Energy Procedia*, *125*, pp. 561—570.

DOI: http://doi.org/10.1016/j.egypro.2017.08.195

Available online at www.sciencedirect.com

ScienceDirect

Energy Procedia 125 (2017) 561–570

Energy Procedia

www.elsevier.com/locate/procedia

European Geosciences Union General Assembly 2017, EGU Division Energy, Resources & Environment, ERE

# Predicting macroscopic elastic rock properties requires detailed information on microstructure

Maria Wetzel[a,*], Thomas Kempka[a] and Michael Kühn[a,b]

[a]*GFZ German Research Centre for Geosciences, Fluid Systems Modelling, Telegrafenberg, 14473 Potsdam, Germany*
[b]*University of Potsdam, Institute of Earth and Environmental Science, Karl-Liebknecht-Str. 24-25, 14476 Potsdam, Germany*

**Abstract**

Predicting variations in macroscopic mechanical rock behaviour due to microstructural changes, driven by mineral precipitation and dissolution is necessary to couple chemo-mechanical processes in geological subsurface simulations. We apply 3D numerical homogenization models to estimate Young's moduli for five synthetic microstructures, and successfully validate our results for comparable geometries with the analytical Mori-Tanaka approach. Further, we demonstrate that considering specific rock microstructures is of paramount importance, since calculated elastic properties may deviate by up to 230 % for the same mineral composition. Moreover, agreement between simulated and experimentally determined Young's moduli is significantly improved, when detailed spatial information are employed.


Peer-review under responsibility of the scientific committee of the European Geosciences Union (EGU) General Assembly 2017 – Division Energy, Resources and the Environment (ERE).

*Keywords:* digital rock physics; effective elastic properties; numerical homogenization, Young's modulus, micromechanics, geomaterials

## 1. Introduction

Prediction of macroscopic mechanical rock properties based on their microstructure and mineralogical composition has a wide practical importance. Particularly regarding changes due to thermal or chemical processes within the context of risk assessments for various types of subsurface utilization or improving the understanding of

* Corresponding author. Tel.: +49 331 288 28669; Fax: +49 331 288 1529.
*E-mail address:* maria.wetzel@gfz-potsdam.de

1876-6102 
Peer-review under responsibility of the scientific committee of the European Geosciences Union (EGU) General Assembly 2017 – Division Energy, Resources and the Environment (ERE).
10.1016/j.egypro.2017.08.195

geogenic processes. A variety of homogenization models can be used to relate macroscopic elastic rock behaviour to the mechanical characteristics of its microstructure and mineralogical composition. For a representative elementary volume (REV), effective elastic properties can be determined, e.g., by analytical homogenization methods. The first approaches by Voigt [1] and Reuss [2] predict upper and lower strength bounds by averaging elastic rock parameters of the mineralogical components. Many mean-field homogenization schemes consider inclusion geometries based on the Eshelby solution [3] of an ellipsoidal inhomogeneity embedded in an infinite medium. In this context, most popular concepts are the dilute scheme [4], the self-consistent approximation [5], the differential scheme [6] as well as the Mori-Tanaka approach [7]. Further models consider certain types of rocks, characterized by a particular microstructure [8,9]. However, none of the analytical models can determine elastic rock parameters for complex multi-component systems and the full range of possible pore network geometries.

Several numerical approaches are employed to estimate rock elasticity, either for synthetic geometries finding an adequate specific analytical solution [10,11] or to improve the understanding of geological processes at REV scale [12]. Characteristic microstructures derived from digital images are taken into account within the field of digital rock physics to estimate permeability, conductivity or effective elastic moduli [13–15]. Despite their higher computational demand in comparison to analytical methods, numerical models provide significant benefits, including consideration of various rock types and their characteristic microstructures. Also, these models can be extended for internal stresses occurring within the rock matrix due to swelling, shrinking, crystallization or changes in pore fluid pressure. Additionally, the presented approach allows for chemo-mechanical coupling within a simulation framework [16]: elastic rock properties can be determined depending on chemical changes, such as mineral dissolution and precipitation, and further upscaled from REV to reservoir scale (Fig. 1). This kind of approach is of particular relevance, since a direct chemo-mechanical feedback is rarely considered in studies regarding subsurface process assessments [17,18], while spatial heterogeneity at different scales significantly affects geochemistry, and thus reactive transport [19].

The calculated rock properties depend on three essential input parameters: (1) elastic properties and (2) volume fractions of the mineral components as well as (3) microstructure of the inclusions. This study particularly investigates the effects of (2) and (3), comparing a widely-used analytical approach with a numerical one. For a range of elastic rock parameters, the presented numerical homogenization model considers five different inclusion geometries to examine the impact of the microstructure. Moreover, elastic parameters of the synthetically generated geometries are modelled and compared with experimental data from the literature, considering the same mineralogical rock composition. Aim of this study is to determine the main influencing factors of the numerical estimation of macroscopic elastic rock properties.

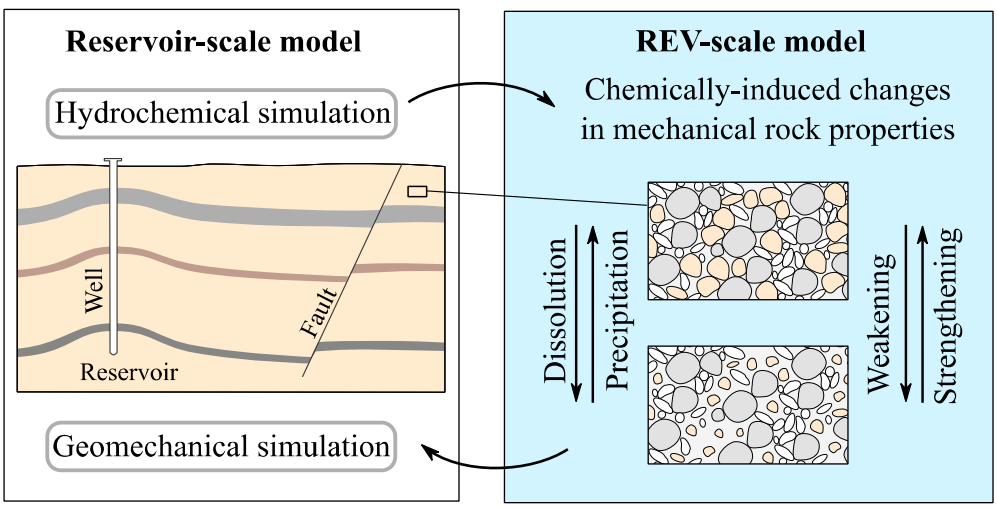


Fig. 1. Prediction of macroscopic mechanical rock properties based on their microstructure within the concept of chemo-mechanical coupling: changes in mineralogical composition can significantly strengthen or weaken rocks.

## 2. Analytical and numerical homogenization models

### *2.1. Mori-Tanaka approach for spherical inclusions*

The Mori-Tanaka solution is one of the most frequently used mean-field homogenization schemes for composite materials. Since the dilute scheme [4] neglects any mechanical interaction between neighbouring inclusions and self-consistent approximation [5] does not define a clear matrix phase, this approach is chosen to analytically calculate the elastic rock parameters. The Mori-Tanaka model is employed within the field of material sciences, but also in geosciences to assess geomechanical properties depending on pore shapes and orientations [10,20,21], and fractures [22,23] as well as for elastic parameter determination of realistic rocks [11,24]. It offers a fast estimation on how material compositions change elastic properties, e.g., rock weakening due to an increase in porosity (Fig. 2).

The commonly used version of the Mori-Tanaka method was reformulated by Benveniste [25]. He assumed that each inhomogeneity is embedded in an infinite matrix. The interaction between single inclusions is taken into account by applying an effective uniform matrix strain to each inclusion. The stiffness tensor of the composite can be calculated, considering the stiffness of the matrix $C_0$ and its inclusions $C_i$, as given in Equation 1:

$$C_{effective} = C_0 + \sum_{i=1} f_i (C_i - C_0) A_i \tag{1}$$

with the volume fractions of the matrix and the inclusions represented by $f_0$ and $f_i$, respectively. The strain-localization tensor $A_i$ is given by Equations 2 and 3:

$$A_i = T_i \left[ f_0 I + \sum_{j=1} f_j T_i \right]^{-1} \tag{2}$$

$$T_i = \left[ I + S_i C_0^{-1} (C_i - C_0) \right]^{-1} \tag{3}$$

where $I$ illustrates the fourth order identity tensor. The calculation of tensor $T$ includes the Eshelby tensor $S_i$, which depends on the shape of the ellipsoid and Poisson's ratio of the matrix $v_0$. Mathematical expressions for several ellipsoidal inclusion shapes can be found in Mura [26]. For the assumed spherical shape of the inclusion, the fourth order Eshelby tensor has the compact mathematical expression given in Equation 4:

$$S_{ijkl} = \frac{5v_0 - 1}{15(1 - v_0)} \delta_{ij}\delta_{kl} + \frac{4 - 5v_0}{15(1 - v_0)} (\delta_{ik}\delta_{jl} + \delta_{il}\delta_{jk}) \tag{4}$$

where the indices *ijkl* denote the position of the tensor component. Kronecker delta $\delta$ is equal to one, if the two indices have the same value ($\delta_{ij} = 1$ for $i = j$), otherwise it becomes zero ($\delta_{ij} = 0$ for $i \neq j$). Besides the ellipsoidal geometry, the Mori-Tanaka approach is limited to inclusion volumes up to 30 % and produces imprecise estimations for higher volume fractions [27]. Furthermore, the effective stiffness tensor must be diagonally symmetric, what holds only for binary composites of any shape or multi-component composites of similar geometry and inclusion orientation [28].

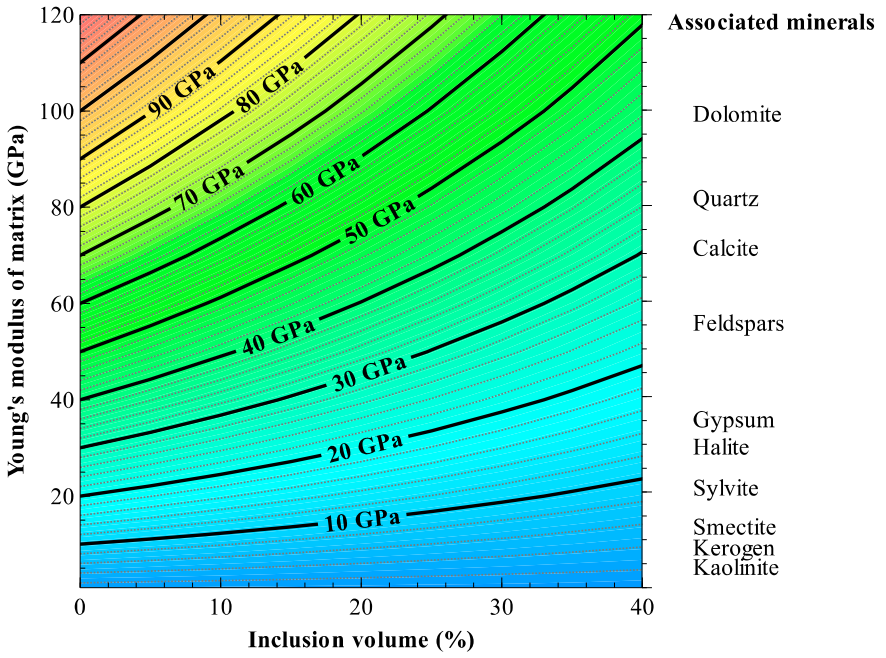


Fig. 2. Mori-Tanaka estimates for a matrix with a range of geologically reasonable Young's moduli and dry spherical pores. The composite's stiffness (hot colours) or softness (cold colours) depends on the inclusion volume fraction as well as Young's moduli of the inclusions and matrix.

### 2.2. *Set up of our numerical models*

Young's moduli are determined by simulating uniaxial compression of a normalized 3D REV-scale cube by means of the finite differences software package FLAC$^{3D}$ [29]. Either uniform normal stress or velocity boundary conditions are applied perpendicular to the top of the model (z = 1), while parallel velocity at the opposite boundary (z = 0) is zero. As illustrated in Fig. 3a, the four remaining boundaries are allowed to move freely in any direction. While an uniform velocity boundary corresponds to an upper bound, a uniform stress boundary results in a lower bound and the elastic modulus of an ideal composite falls in between [30]. Young's modulus (E) and Poisson's ratio (ν) are calculated considering the mean stresses and strains along the boundary faces of the cube. To determine effective elastic parameters for each direction and considering a potential anisotropy, the numerical experiment has to be repeated in the two remaining principle directions. To cover a wide range of geologically reasonable rock properties and clearly indicate microstructural effects, a high contrast for the initial elastic parameter is chosen: quartz as stiff mineral with E = 95.5 GPa and ν = 0.08 and the clay mineral kaolinite as soft component with E = 3.2 GPa and ν = 0.144 [31].

For the normalized REV-scale cube, five different inclusion geometries and spatial mineral distributions are selected to examine the impact of the microstructure: for comparability with the analytical Mori-Tanaka approach, one single sphere as well as non-intersecting randomly distributed spherical inclusions are chosen (Fig. 3). For the latter purpose, 350 spheres are randomly distributed at a minimum distance of 0.005 of the REV-scale cube size to each other. Further, a regular Cartesian grid with randomly distributed cubic inclusions is used for comparison purposes and to increase computational efficiency. A resolution of 30 x 30 x 30 elements is employed, since Young's modulus was found not to vary with higher grid discretization for the employed models. A synthetic pore network and a layering of four distinct layers are selected to represent geological microstructures. The pore network is generated by intersection of randomly distributed spheres in a rock matrix. In this case, grid resolution has to be relatively high to capture the microstructures in detail.

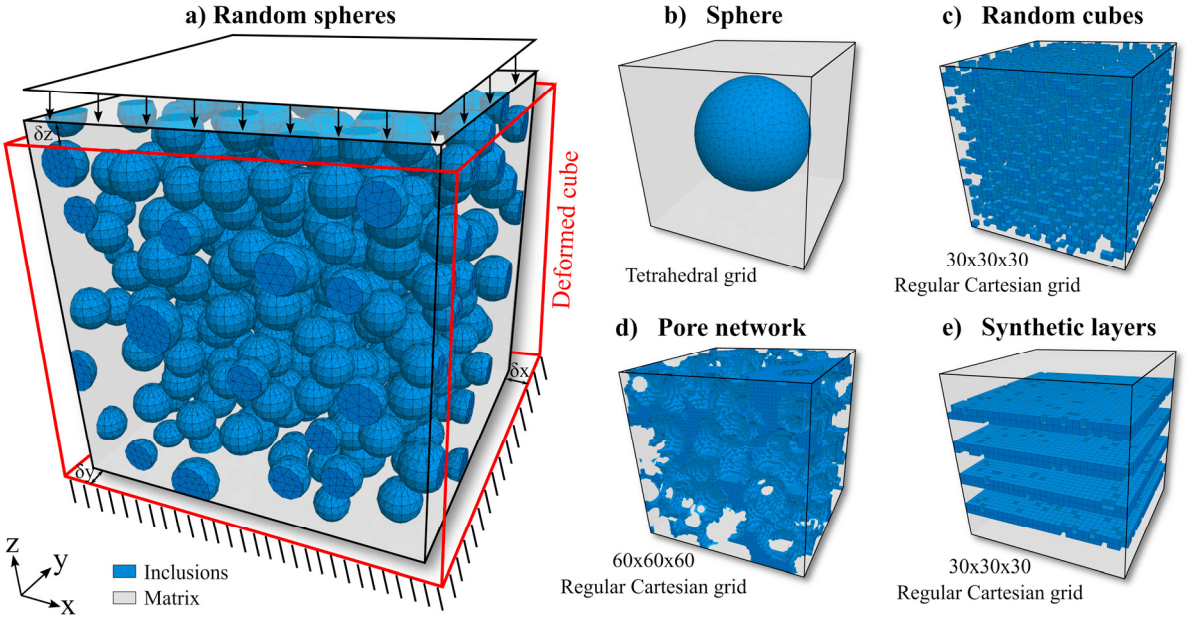


Fig. 3. Normalized REV cube with five inclusion types of 25 % inclusion volume each. (a) Young's modulus and Poisson's ratio are calculated based on the mean stresses and strains at the boundary faces, resulting from uniaxial compression. While inclusion geometries (a,b,c) are selected to enable comparison with the analytical solution, subfigures d) and e) represent synthetic geological geometries.

## 3. Results and discussion

### *3.1. Validation of numerical simulation results against Mori-Tanaka approach*

For binary mixtures with spherical inclusions, the Mori-Tanaka solution corresponds to the Hashin-Shtrikman upper and lower bounds [32] for the applied matrix materials quartz and kaolinite, respectively (Fig. 4a). Since the Mori-Tanaka approach provides accurate results for porosities of up to 30 % only [27], a broad range of volume fractions cannot be addressed by it. Also, the numerical approach with one spherical inclusion is limited by geometric restrictions, as the sphere intersects model boundaries when a pore volume of 52 % is achieved.

The simulation results with one or several random spherical inclusions replicate the analytical Mori-Tanaka solution, assuming the same geometry (Fig. 4a). In accordance with the findings of Khisaeva and Ostoja-Starzewski [30], constant stress and constant velocity boundary conditions slightly under- and overestimate the analytical results, respectively (Fig. 4b). Further, the degree of deviation between both approaches depends on the stiffness ratio between the matrix and its inclusions. Random spherical inclusions for a stiff matrix with soft spheres give similar results with a considerably better estimation due to the reduction of boundary effects compared to one large sphere (Fig. 4b). Since there is a minor influence of the inclusion shape on the calculated elastic parameters for one single inclusion [11], our results indicate a significantly stiffer behaviour in case of various randomly distributed cubes. Especially stiff cubic inclusions embedded in a soft matrix lead to an overestimation of the analytical Mori-Tanaka approach by up to 168 % (Fig. 4b), while the deviation amounts only to 10 % for soft inclusions within a stiff matrix. That corresponds to the findings of Belayachi et al. [33], who demonstrated that inclusion morphology impacts the estimated elastic properties, particularly for stiff mineral inclusions.

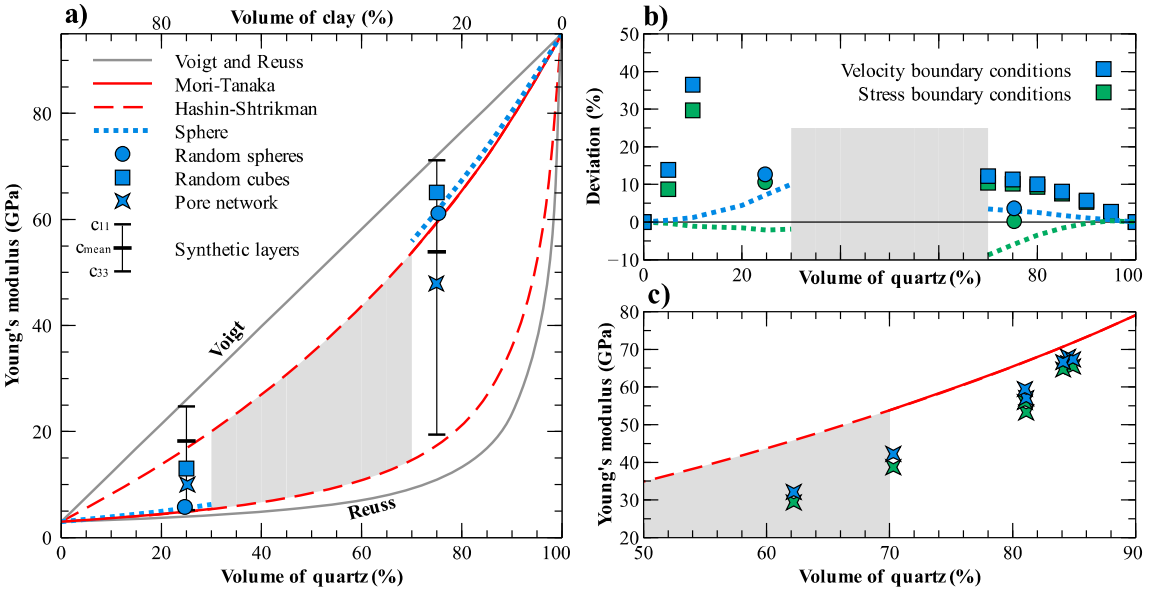


Fig. 4. (a) Numerical estimations for several synthetic geometries and reasonable geologic microstructures compared against analytical solutions. The range beyond reliable Mori-Tanaka estimations is displayed in grey. (b) Deviation from the Mori-Tanaka solution depending on the boundary conditions. (c) Analytical solution overestimates elasticity considering a pore network as microstructure.

Considering the synthetic pore network as a more geologically reasonable geometry to represent sedimentary rocks, the analytical Mori-Tanaka solution overestimates rocks elasticity by 39 % for the of 30 % inclusion volume (Fig. 4 c). A distinct layering within the rock leads to a strong anisotropic behaviour: the rock behaves stiffer in parallel direction to the bedding and weaker perpendicular to it. Regarding the mean Young's modulus compared to an isotropic distribution, the composite is weakened by up to 17 % and strengthened by up to 40 % for a quartz and clay matrix, respectively (Fig. 4a). The absolute deviations between the five investigated geometries are 12.9 GPa and 17.2 GPa regarding clay and quartz matrices, respectively. Considering a distinct layering of stiff inclusions within soft matrix affects the Young's modulus by up to 230 %, compared to random spherical inclusions.

The reason for the presented variations in the estimated Young's moduli is the difference in stress distribution in the considered microstructures. As shown in Fig. 5, pore network shape and arrangement significantly impact the internal stress distribution: for synthetic spherical and cubic geometries, stress is relatively uniformly distributed, while stress is considerably localized for more geologically representative geometries. Hence, the rock's microstructure is of significant importance and has to be considered carefully taking into account the particular rock.

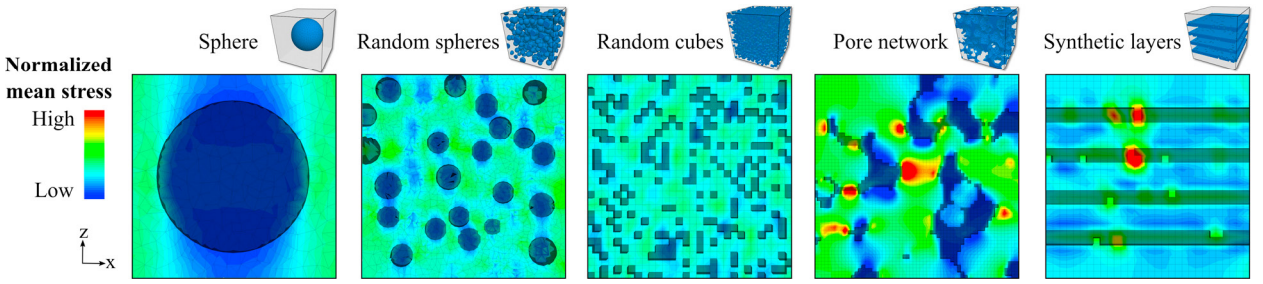


Fig. 5. Cross-section trough the centre of the REV cube displays the differences in the internal stress regime depending on the five considered microstructures. The stiff matrix consists of quartz, while inclusions are composed of soft clay minerals. Compression is uniaxial in z-direction.

### 3.2. Comparison of the numerical simulation results against experimental data

The next step includes the comparison of our numerical approach with published data, whereby mineralogical rock compositions and experimentally determined elastic properties are given. A summary of typical values for elastic parameters of common rock constituents is provided in Table 1, and the compositions of all examined rocks are plotted in Fig. 6c. All rocks are considered as dry in our models to enable a comparison with the experimental data. An excellent match is found for granite, since its microstructure is probably well represented by an isotropic distribution of random cubes. For sedimentary rocks composed of specific grains and a distinct pore network, as sandstones and carbonates, an isotropic distribution is not suitable to determine elastic rock properties, since it results in an overestimation. Using a synthetic pore network considerably improves matching with experimentally determined Young's moduli, reducing the deviation for the Fontainebleau sandstone from 57 % for an isotropic distribution to 30 % when considering a synthetically generated pore network instead (Fig. 6a). Andrä et al. [14] used digital images and were able to further improve the agreement with the calculated elastic modulus, exceeding the experimental one [34] by only 19 %. This approach cannot be transferred to shales, where numerical models overestimate (Haddessen and Harderode shale [35]) and underestimate (Kimmeridge and Jurassic shale [36]) given experimental data (Fig. 6b), respectively. Rybacki et al. [35] postulate that for the Haddessen and Harderode shales a correlation between the elastic modulus and the rock's carbonate contents is not evident. Since these shales exhibit a comparably high amount of carbonate, behaving relatively stiff in our numerical model, this may be one reason for the Young's modulus overestimation. However, improving our match without precise microstructural information, especially on the spatial distribution of the rock's mineral components is impossible.

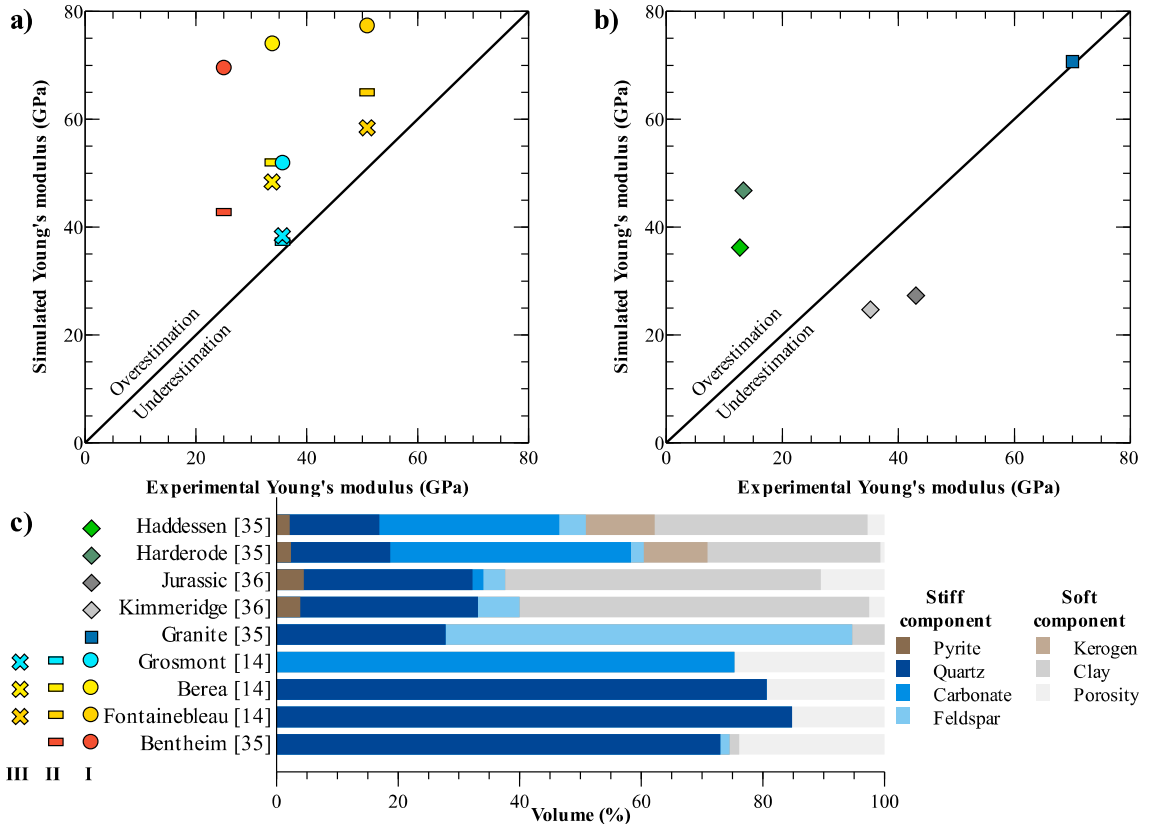


Fig. 6. Comparison of simulated and experimental Young's moduli [34–36] for (a) sandstones and carbonates with different microstructures: (I) isotropic, (II) pore network and (III) digital image calculated by Andrä et al. [14] as well as (b) shales and granite. (c) Mineralogical composition of the selected rocks.

Moreover, expecting a complete match between simulated and experimentally determined elastic properties is not expedient for several reasons: quality of our numerical results is affected by model parametrization, since elastic properties of individual minerals can significantly vary, e.g., Young's modulus of feldspars is in the range of 61.3 GPa (orthoclase) to 89.2 GPa (anorthite) [37]. Further, it is not always known if the respective minerals are crystallized or precipitated in an amorphous phase, whereby the latter would considerably reduce their elastic properties. In general, predicting rock properties by numerical simulations requires an accurate description of the spatial mineral distribution in the REV, as the number of grain contacts is a key parameter for this undertaking [38].

Table 1. Young's moduli and Poisson's ratios for constituents of the investigated rocks.

| Constituent | Young's modulus (GPa) | Poisson's ratio (-) | Reference |
|---|---|---|---|
| Pyrite | 291.5 | 0.16 | Bass et al. [37] |
| Quartz | 95.5 | 0.08 | Bass et al. [37] |
| Calcite | 80.7 | 0.32 | Mavko et al. [31] |
| Albite | 73.4 | 0.285 | Bass et al. [37] |
| Kerogen | 6.1 | 0.145 | Mavko et al. [31] |
| Kaolinite | 3.2 | 0.144 | Mavko et al. [31] |

## 4. Conclusions and Outlook

We applied a numerical REV-scale model to determine macroscopic elastic rock properties based on their microstructure and mineralogical composition. Our numerical modelling approach was successfully validated against the analytical Mori-Tanaka model for comparable geometries and a range of geologically reasonable elastic parameters. The paramount importance of considering the detailed rock microstructure was shown by employing three simple inclusion geometries and two geologically reasonable microstructures, including pore networks and synthetic layering models. The investigated geometries affect the determined Young's modulus up to 26 % and 230 % considering quartz and clay matrices, respectively. Hence, the inclusion shape is of particular importance for stiff minerals embedded in soft matrices. Especially for the synthetic pore network, the analytical Mori-Tanaka solution overestimated rocks elasticity by 39 % for a 30 % inclusion volume, and is therefore of limited suitability for prediction of elastic properties of sedimentary rocks.

Matching of simulated and experimental Young's moduli depends on the respective rock type and the representation of its particular microstructure. As we demonstrated, prediction of macroscopic elastic rock properties was improved for sandstones from 57 % to 30 % by using a synthetically generated pore network. Since this study mainly investigated the effect of rock composition and microstructure, the calculated elastic properties further depend on model parametrization. For instance, elastic properties of individual minerals can significantly vary, depending on mineral type and if it is crystallized or precipitated in an amorphous phase.

Despite the higher computational demand of the numerical approach compared to the analytical Mori-Tanaka solution, it provides significant benefits such as the flexibility in implementing different non-spherical microstructures as well as effects, including fluid pressure as well as mineral shrinking and swelling. Chemically-induced changes affecting elastic rock behaviour are of importance for several processes occurring in subsurface utilization [39–41], but are rarely considered so far [42–44]. Hence, our presented approach is of high relevance for the development of sequentially coupled chemo-mechanical models, since it allows to estimate changes in elastic rock behaviour due to chemically-induced changes in mineralogical composition and rock microstructure.

## References


[1] Voigt, W. (1889) "Über die Beziehung zwischen den beiden Elasticitätsconstanten isotroper Körper." Annalen Der Physik 274: 573–587.
[2] Reuss, A. (1929) "Berechnung der Fliessgrenze von Mischkristallen auf Grund der Plastizitätitsbedingung für Einkristalle." Zeitschrift Für Angewandte Mathematik und Mechanik 9: 49–58.
[3] Eshelby, J. (1957) "The determination of the elastic field of an ellipsoidal inclusion, and related problems." Mathematical, Physical and Engineering Sciences 241: 376–396.
[4] Withers, P., Stobb, W., Pedersen, O. (1989) "The Application of the Eshelby Method of Internal Stress Determination to Short Fiber Metal Matrix Composites." Acta Metallurgica 37: 3061–3084.
[5] Hill, R. (1965) "A self-consistent mechanics of composite materials." Journal of the Mechanics and Physics of Solids 13: 213–222.
[6] McLaughlin, S. (1977) "Electrostatic Potentials at Membrane-Solution Interfaces." Current Topics in Membranes and Transport 9: 71 144.
[7] Mori, T., Tanaka, K. (1973) "Average stress in matrix and average elastic energy of materials with misfitting inclusions." Acta Metallurgica 21: 571–574.
[8] Backus, G. (1962) "Long-wave elastic anisotropy produced by horizontal layering." Journal of Geophysical Research 67: 4427–4440.
[9] Hudson, J. (1979) "Overall properties of a cracked solid." Mathematical Proceedings of the Cambridge Philosophical Society 88: 371 384.
[10] Suvorov, A., Selvadurai, A. (2011) "Effective medium methods and a computational approach for estimating geomaterial properties of porous materials with randomly oriented ellipsoidal pores." Computers and Geotechnics 38: 721–730.
[11] Goodarzi, M., Rouainia, M., Aplin, A.C. (2016) "Numerical evaluation of mean-field homogenisation methods for predicting shale elastic response." Computational Geosciences 20: 1109–1122.
[12] Sain, E., Mukerji, T., Mavko, G. (2014) "How computational rock-physics tools can be used to simulate geologic processes, understand pore-scale heterogeneity, and refine theoretical models." The Leading Edge 33: 324–334.
[13] Arns, C., Knackstedt, M., Pinczewski, W., Garboczi, E. (2002) "Computation of linear elastic properties from microtomographic images: Methodology and agreement between theory and experiment." Geophysics 67: 1396–1405.
[14] Andrä, H., Combaret, N., Dvorkin, J., Glatt, E., Han, J., Kabel, M., Keehm, Y., Krzikalla, F., Lee, M., Madonna, C., Marsh, M., Mukerji, T., Saenger, E.H., Sain, R., Saxena, N., Ricker, S., Wiegmann, A., Zhan, X. (2013) "Digital rock physics benchmarks-part II: Computing effective properties." Computers and Geosciences 50: 33–43.
[15] Saenger, E., Vialle, S., Lebedev, M., Uribe, D., Osorno, M., Duda, M., Steeb, H. (2016) "Digital carbonate rock physics." Solid Earth 7: 1185–1197.
[16] Kempka, T., Nakaten, B., De Lucia, M., Nakaten, N., Otto, C., Pohl, M., Tillner, E. (2016) "Flexible Simulation Framework to Couple Processes in Complex 3D Models for Subsurface Utilization Assessment." Energy Procedia 97: 494–501.
[17] De Lucia, M., Kempka, T., Kühn, M. (2015) "A coupling alternative to reactive transport simulations for long-term prediction of chemical reactions in heterogeneous CO2 storage systems." Geoscientific Model Development 8: 279–294.
[18] Kempka, T., De Lucia, M., Kühn, M. (2014) "Geomechanical integrity verification and mineral trapping quantification for the Ketzin CO2 storage pilot site by coupled numerical simulations." Energy Procedia 63: 3330–3338.
[19] De Lucia, M., Lagneau, V., de Fouquet, C., Bruno, R. (2011) "The influence of spatial variability on 2D reactive transport simulations." Comptes Rendus - Geoscience 343: 406–416.
[20] Giraud, A., Hoxha, D., Do, D., Magnenet, V. (2008) "Effect of pore shape on effective porothermoelastic properties of isotropic rocks." International Journal of Solids and Structures 45: 1–23.
[21] Vernik, L., Kachanov, M. (2010) "Modeling elastic properties of siliciclastic rocks." Geophysics 75: E171–E182.
[22] Teng, H. (2013) "Prediction of the effective Young's modulus of a particulate composite containing fractured particles." Finite Elements in Analysis and Design 65: 32–38.
[23] Marmier, R., Jeannin, L., Barthélémy, J. (2007) "Homogenized constitutive laws for rocks with elastoplastic fractures." International Journal for Numerical and Analytical Methods in Geomechanics 31: 1217–1237.
[24] Abou-Chakra Guéry, A., Cormery, F., Shao, J., Kondo, D. (2010) "A comparative micromechanical analysis of the effective properties of a geomaterial: Effect of mineralogical compositions." Computers and Geotechnics 37: 585–593.
[25] Benveniste, Y. (1987) "A new approach to the application of Mori-Tanaka's theory in composite materials." Mechanics of Materials 6: 147–157.
[26] Mura, T. (1987) "Micromechanics of defects in solids", Martinus Nijhoff Publishers Dordrecht, The Netherlands.
[27] Parsaee, A., Shokrieh, M.M., Mondali, M. (2016) "A micro-macro homogenization scheme for elastic composites containing high volume fraction multi-shape inclusions." Computational Materials Science 121: 217–224.
[28] Benveniste, Y., Dvorak, G., Chen, T. (1991) "On diagonal and elastic symmetry of the approximate effective stiffness tensor of heterogeneous media." Journal of the Mechanics and Physics of Solids 39: 927–946.
[29] Itasca (2014) FLAC3D Software Version 5.0. User's Manual. Advanced Three-Dimensional Continuum Modelling for Geotechnical Analysis of Rock, Soil and Structural Support.
[30] Khisaeva, Z., Ostoja-Starzewski, M. (2006) "On the Size of RVE in Finite Elasticity of Random Composites." Journal of Elasticity 85: 153–173.
[31] Mavko, G., Mukerji, T., Dvorkin, J. (2009) "The rock physics handbook: Tools for seismic analysis of porous media", Cambridge University Press, Cambridge.
[32] Hashin, Z., Shtrikman, S. (1962) "A variational approach to the elastic behavior of multiphase materials." Journal of the Mechanical Physics of Solids 11: 127–140.

[33] Belayachi, N., Do, D., Hoxha, D. (2012) "A note on the numerical homogenisation of the mechanical behaviour of an argillaceous rock." Computers and Geotechnics 41: 70–78.
[34] Han, D.Effects of porosity and clay content on acoustic properties of sandstones and uncosolidated sediments, Stanford University, 1986.
[35] Rybacki, E., Meier, T., Dresen, G. (2015) "What controls the mechanical properties of shale rocks? - Part II: Brittleness." Journal of Petroleum Science and Engineering 144: 39–58.
[36] Hornby, B. (1998) "Experimental laboratory determination of the dynamic elastic properties of wet, drained shales." Journal of Geophysical Research 103: 945–964.
[37] Bass, J. (1995) "Elasticity of Minerals, Glasses, and Melts" in Ahrens (eds) Mineral physics & crystallography: a handbook of physical constant, American Geophysical Union.
[38] Cook, J., Goodwin, L., Boutt, D., Tobin, H. (2015) "The effect of systematic diagenetic changes on the mechanical behavior of a quartz-cemented sandstone." Geophysics 80: D145–D160.
[39] Tillner, E., Langer, M., Kempka, T., Kühn, M. (2016) "Fault damage zone volume and initial salinity distribution determine intensity of shallow aquifer salinisation in subsurface storage." Hydrology and Earth System Sciences 20: 1049–1067.
[40] Jacquey, A.B., Cacace, M., Blöcher, G., Scheck-Wenderoth, M. (2015) "Numerical Investigation of Thermoelastic Effects on Fault Slip Tendency during Injection and Production of Geothermal Fluids." Energy Procedia 76: 311–320.
[41] Ballarini, E., Graupner, B., Bauer, S. (2017) "Thermal- hydraulic - mechanical behavior of bentonite and sand-bentonite materials as seal for a nuclear waste repository: Numerical simulation of column experiments." Applied Clay Science 135: 289–299.
[42] Taron, J., Elsworth, D. (2010) "Coupled mechanical and chemical processes in engineered geothermal reservoirs with dynamic permeability." International Journal of Rock Mechanics and Mining Sciences 47: 1339–1348.
[43] Zhang, R., Yin, X., Winterfeld, P.H., Wu, Y.S. (2016) "A fully coupled thermal-hydrological-mechanical-chemical model for CO2 geological sequestration." Journal of Natural Gas Science and Engineering 28: 280–304.
[44] Zheng, L., Rutqvist, J., Birkholzer, J., Liu, H. (2015) "On the impact of temperatures up to 200°C in clay repositories with bentonite engineer barrier systems: A study with coupled thermal, hydrological, chemical, and mechanical modeling." Engineering Geology 197: 278 295.